HIGH FREQUENCY CAPACITANCES DETERMINATION IN THREE-PHASE PWM INVERTER-MOTOR DRIVE SYSTEM USING AN ALTERNATIVE METHOD APPLIED TO EMI EFFECT STUDIES

Rudolf Ribeiro Riehl[(1)] Ernesto Ruppert Filho[(2)]
(1) São Paulo State University – Unesp - Bauru
(2) State University of Campinas – Unicamp - Campinas
(1) *rrriehl@feb.unesp.br*; (2) *ruppert@fee.unicamp.br*

***Abstract*- The aim of this paper is to present a simple method for determining the high frequency capacitances of a three-phase induction motor to be used in studies involving variable speed drives with PWM three-phase inverters, in which it is necessary to check the effects caused to the motor by the electromagnetic interference, (EMI) in the differential mode, as well as in the common mode. The motor parameters (R, L and C) determination is generally performed in adequate laboratories using accurate instruments, such as very expensive RLC bridges. The method proposed here consists in the identification of the motor equivalent electrical circuit parameters in rated frequency and in high frequency (capacitances) through characteristic tests in the laboratory, together with the use of characteristic equations and curves, shown in the references to be mentioned for determining the motor high frequency parasite capacitances and also through system simulations using dedicated software, like Pspice, determining the characteristic waveforms involved in the differential and common mode phenomena, comparing and validating the procedure through published papers [01].**

***Keywords* – Electromagnetic Interference; Induction Motor; Pspice; PWM Inverter.**

I – INTRODUCTION

Three-phase induction motor variable speed drives are widely used today in the entire world mainly in the range of 10 Hp powers.

The recent development of power electronic devices, such as IGBT, MOSFET and GTO causes the increase of their switching frequency reaching easily 20 kHz. The high values of the switching frequencies are responsible for the presence of emi problems in induction motors due to the parasite capacitances, which create paths to the high frequency electrical current circulation among motor phase windings (differential mode) and between motor phase windings and ground (common mode) causing nonzero common voltages. The larger the switching frequencies more severe will be those phenomena.

The emi differential mode phenomena are responsible for the excessive motor heating, thus damaging the electrical insulation, decreasing the motor efficiency and consequently shortening the useful life of the motor. This occurs because the inverter motor input voltages are not sinusoidal due to the switching effects, thus causing high values of dV/dt to be applied to the stator motor windings.

The phenomena, due to the common mode emi, are responsible for the rising of circulation current between the motor windings and the ground through the bearings and shaft (bearing currents), that can damage the bearing internal surfaces and the shat external surface causing, eventually, rotor locking. Another possible phenomenon is the appearance of voltage, between the motor frame and shaft, which is known as shaft voltage and is dependent on the common mode voltage, as well as the parasitic winding capacitances. It is responsible for the electrical discharge machine (EDM) when the motor is grounded.

The most used method for determining those capacitances is the induction machine impedance measurement using RLC bridges. There are several types of measurements to determine the high frequency motor electrical equivalent circuit, as shown in [01, 02, 03, 04, 07].

The proposal of this paper is to develop a simplified method consisting of the determination of the motor equivalent electrical circuit parameters through the characteristic tests performed in laboratory for the low frequency parameters determination, in the use of characteristic equations and curves for determining the motor high frequency parasite capacitances of the high frequency model of the induction motor [02, 03, 04] and also through system (three-phase induction machine motor fed from PWM inverter with high frequency equivalent electrical circuit) simulations using dedicated software, such as Pspice determining the characteristic waveforms involved in the differential and common mode phenomenon comparing and validating the procedure through published paper results [01].

The induction motor used in this paper is a 3.7kW (5hp) three-phase induction motor fed from a three-phase PWM inverter using V/Hz to control the motor speed. The waveforms method results obtained in this paper are compared with those in [01] to validate this procedure.

II – THE PROCEDURE PROPOSAL

II.a – Low Frequency Induction Motor Equivalent Electrical Circuit Parameters

The two wattmeters method are used in the no-load, as well as in the blocked-rotor tests. These tests were performed at the frequency of 50 Hz to permit comparisons with the results obtained by Akagi in [01].

Induction motor data are: rated power: 5Hp (3.7kW), rated voltage: 200V/50Hz (Δ), pole number: 4, rated current: 13.8 A, rated speed: 1715 rpm.

Table I shows the results for the no-load and blocked rotor tests. The phase values of voltage and current are shown.

TABLE I
Induction motor test results

V_O(V)	I_O(A)	P_O(W)	N_O(rpm)
200	2.1	63.33	1798
V_{bl}(V)	I_{bl}(A)	P_{bl}(W)	R_1(Ω)
41	8.0	145.83	1.5

To obtain the equivalent electrical circuit the following equations (per phase) are used:

No-load test

$$R_{Of} = \frac{P_{Of}}{I_{Of}^2}$$
$$Z_{Of} = \frac{V_{Of}}{I_{Of}} \quad (1)$$
$$X_{Of} = \sqrt{Z_{Of}^2 - R_{Of}^2}$$

Blocked-rotor test

$$R_{bf} = \frac{P_{bf}}{I_{bf}^2}$$
$$Z_{bf} = \frac{V_{bf}}{I_{bf}} \quad (2)$$
$$X_{bf} = \sqrt{Z_{bf}^2 - R_{bf}^2}$$

The parameters of the motor equivalent electrical circuit can be calculated by equations (3) and the results are shown in Table II.

$$R_2' = R_{bf} - R_1$$
$$X_1 \cong X_2 = \frac{X_{bf}}{2} \quad (3)$$
$$X_{mag} = X_{Of} - X_1$$

TABLE II
Parameters of the motor equivalent electrical circuit at the frequency of 50 Hz

R_1(Ω)	R_2'(Ω)	$X_1 = X_2$ (Ω)/ $L_1 = L_2$ (mH)	X_{mag}(Ω)/ L_{mag}(mH)
1.5	0.78	2.3/6.1	91.85/243.63

The per fase induction motor equivalent electrical circuit, which was used for calculations and simulations with the results compared with the same results obtained in [01], is shown bellow in Fig.1.

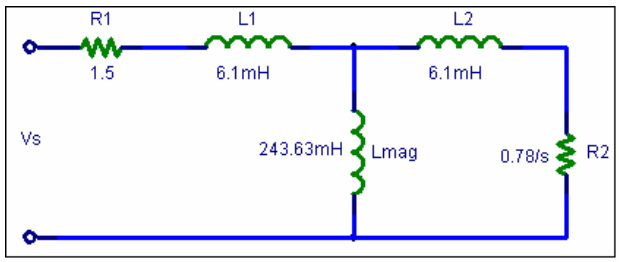

Fig. 1: Parameters of the motor equivalent electrical circuit.

II.b - High Frequency Induction Motor Equivalent Electrical Circuit Parameters

In Fig. 2 the high frequency induction motor equivalent electrical circuit is shown [03, 06].

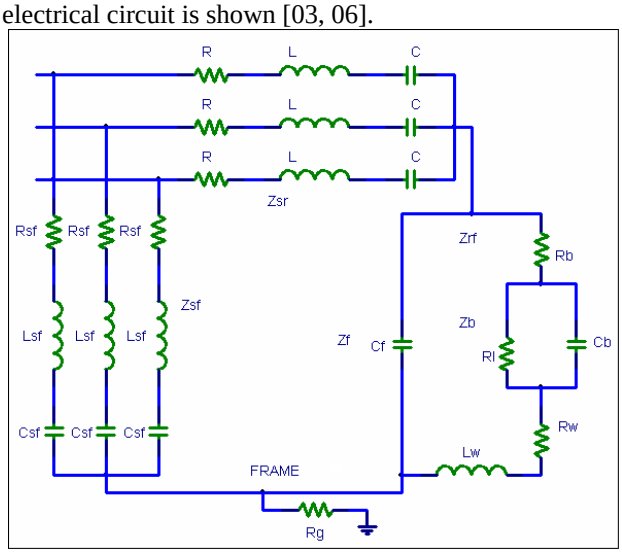

Fig. 2: High frequency motor equivalent electrical circuit.

In this case it has:

$$Z_{rf} = Z_g // Z_b$$
$$Z_b = R_l // XC_b + R_b + R_w + XL_w \quad (4)$$
$$Z_f = XC_f$$
$$Z_{sr} = R + XL + XC$$

In which: Z_{rf} is the impedance between the phase rotor winding and the motor frame, Z_{sr} is the impedance between the phase stator and rotor windings, Z_{sf} is the impedance between the phase stator winding and the frame, Z_g is the air-gap impedance and Z_b is the impedance between the rotor winding and the bearings.

As the three-phase induction motor is not fed from sinusoidal three-phase voltages by the PWM inverter, thus the common mode voltage (Vcm) is not zero and it is dependent on the switching of the power semiconductor devices of the inverter.

$$V_{CM} = \frac{V_a + V_b + V_C}{3} \quad (5)$$

In which V_a, V_b and V_c are the phase voltages generated by the PWM inverter.

The voltage appearing between the motor shaft and its frame (Vshaft) is dependent either on this voltage or on the high frequency impedances as it can be seen in (6).

$$V_{SHAFT} = V_{CM} = \left[\frac{Z_{rf}}{\frac{Z_{sr}}{3} + Z_{rf}} \right] \quad (6)$$

Figure 3 presents the simulated common mode voltage (V_{CM}) and shaft voltage (V_{SHAFT}) for the proposed procedure.

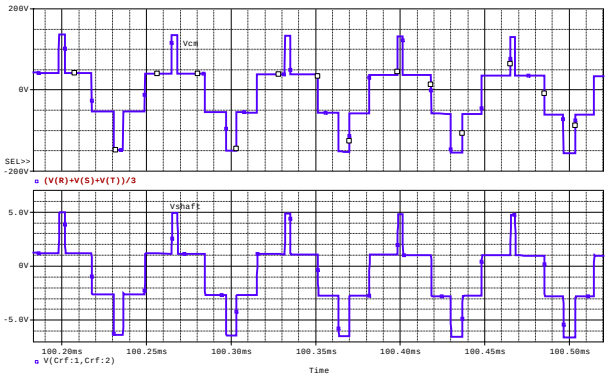

Fig. 3: Common mode voltage (V_{CM}) and shaft voltage (V_{SHAFT}).

The electrical current circulating in the motor bearings, named bearing current, is given by:

$$I_b = \frac{V_{SHAFT}}{Z_b} \quad (7)$$

The leakage electrical current is given by

$$I_C = \frac{V_{CM}}{Z_{rf}/3} + \frac{V_{SHAFT}}{Z_g} + \frac{V_{SHAFT}}{Z_b} = I_{R_g} \quad (8)$$

In which R_g is the electrical resistance between the motor frame and the ground.

Simplifications in the electrical circuit of Fig. 2 can be performed considering the following: **a.** Z_g is a capacitive purely impedance; **b.** as Z_b is constituted by a capacitor in parallel with a high electrical resistance, it may be considered as capacitive impedance; **c.** Z_{sr} for frequencies under 200 kHz [01, 07] has capacitive behavior and **d.** Z_{sf} is a series RC circuit.

Under the inverter switching frequencies the motor parasite impedances have capacitive purely characteristic [01, 07, 10], so the high frequency motor equivalent electrical circuit is drastically simplified as it can be seen in Fig.4 and the shaft voltage can be written as shown in (9).

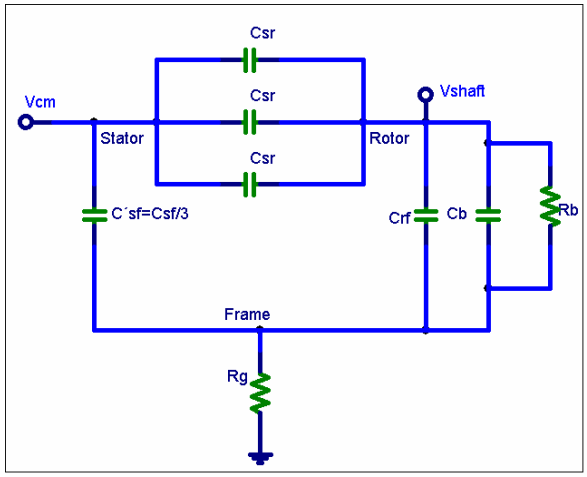

Fig. 4: Simplified high frequency motor equivalent electrical circuit.

$$V_{SHAFT} = V_{CM} \cdot \frac{C'_{sr}}{C'_{sr} + C_{rf} + C_b} \quad (9)$$

In which: $C'_{sr} = C_{sr}/3$

The parasite capacitance values C_{sf}; C_{sr}; C_{rf} e C_b are determined by means of a RLC bridge for a wide range of frequencies [01, 02, 04, 07]. In this paper it is intended to determine and validate this model without using these measurements. The values of these parasite capacitances are obtained from curves showing the capacitance variations in the function of the motor power [02, 03, 04] as shown in Fig. 5a and from the capacitance characteristic equations presented in [03], which show that these parasite capacitances are dependent only on the physical and constructive characteristic of the motor [12] according to Fig. 5b.

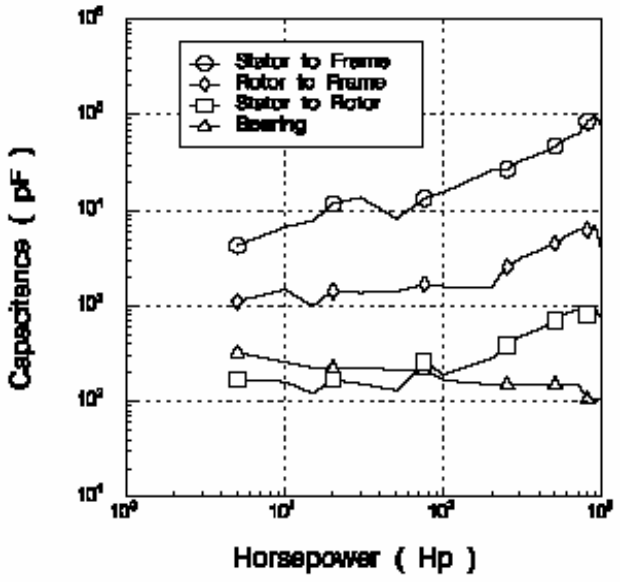

Fig. 5a) Ref.[03] – Figure 4.

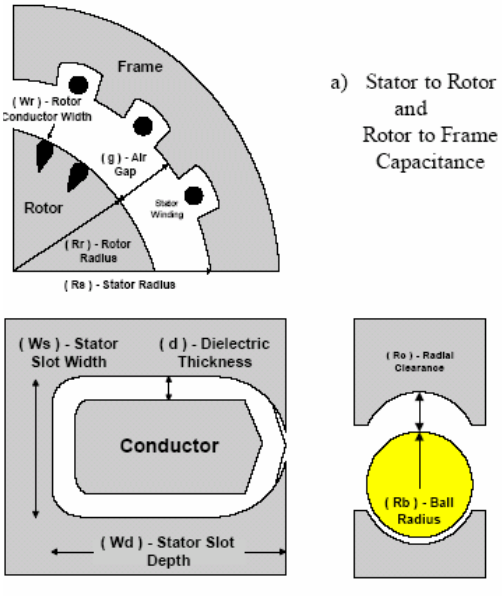

Fig. 5b) Ref.[03] – Figure 3.

The parasite capacitance values for the used motor in this paper are C_{sf} = 4nF; C_{rf} = 1,1nF; C_{sr} = 180pF; C_b = 300pF. In [07, 11] It can be found typical its typical values.

II.c – Pspice implementation of the equivalent electrical circuit

Fig. 8 shows the equivalent electrical circuit implemented in the Pspice, similarly to the presented in [1]. The inverter switching frequency is 15kHz with constant V/Hz and the output frequency is 40Hz.

III – RESULTS AND COMPARISONS

The results of the proposed procedure are presented in the figures below. Voltage and currents waveforms present ideal characteristics (ideal switches) in order to avoid non-convergence situations during simulations, making them faster.

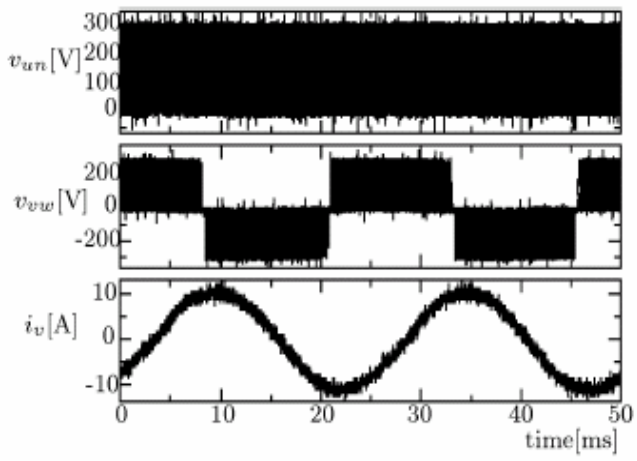

Fig. 6a: Ref. [01] – Figure 6a.

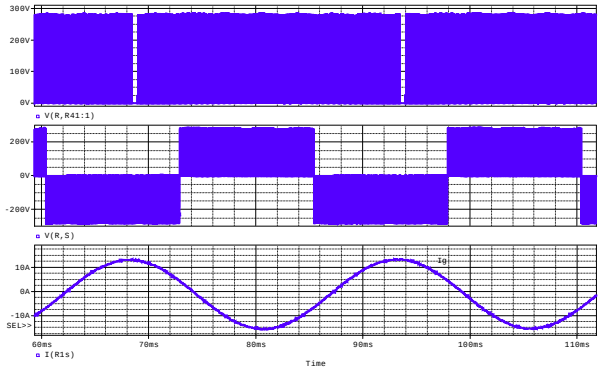

Fig. 6b: Inverter output variables – Phase voltage (V_R); Line voltage (V_{RS}) and Line current (I_R).

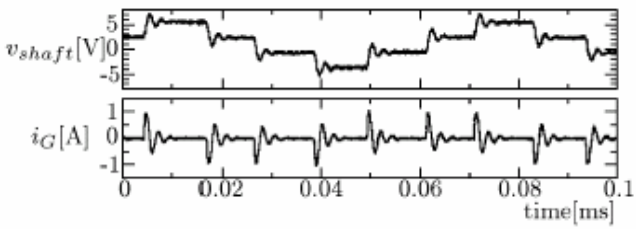

Fig. 7a: Ref. [01] – Figure 6b.

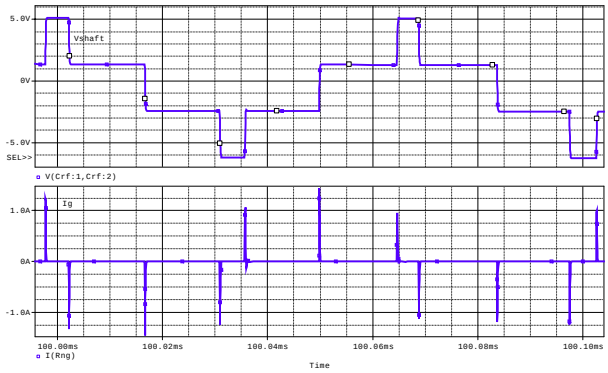

Fig. 7b: Shaft voltage - V_{SHAFT}; Leakage current – I_G.

IV – CONCLUSIONS

The results obtained through the proposed method when compared with the results presented in [01] show that they can be validated and permit to establish a real simplification in the process of the high frequency motor equivalent electrical circuit parameter determination.

On top of that, use of simulation allows to reduce the time elapsed in design of output filters like: dv/dt; sinusoidal; common and differential mode filters to minimize the EMI effects.

V – REFERENCES

[1] H. Akagi, H. Hasegawa, T. Doumoto, “Design and Performance Of A Passive EMI Filter For use With A Voltage-Source PWM Inverter Having Sinusoidal Output Voltage And Zero Common-Mode Voltage”, *IEEE Trans. On Power Electronics*, Vol.19, pp. 1069-1076, Jul. 2004.

[2] D. Busse, J. Erdman, R. J. Kerkman, D. Schlegel, G. Skibinski, "Bearing Currents And Their Relationship To PWM Drives", *IEEE Trans. On Power Electronics*, Vol. 12, pp. 243-252, Mar. 1997.

[3] J. Erdman, R. J. Kerkman, D. Schlegel, G. Skibinski, "System Electrical Parameters And Their Effects On Bearing Currents", *IEEE APEC Conference*, San Jose, CA, Mar. 1996.

[4] J. Erdman, R. J. Kerkman, D. Schlegel, G. Skibinski, "Effect Of PWM Inverters On AC Motor Bearing Currents And Shaft Voltages", *IEEE APEC Conference*, Dallas, TX, Mar. 1995.

[5] S. Ogasawara, H. Akagi, "Modeling And Damping Of High-Frequency Leakage Currents In PWM Inverter-Fed AC Motor Drive Systems", *IEEE Trans. On Industry Applications*, Vol. 32, pp. 1105-1114, 1996.

[6] E. G. Villabona, P. S. Gúrpide, O. A. Sádaba, A. L. Azanza, L. M. Palomo, "Simplified High-Frequency Model For AC Drives", *IEEE 200228th Annual Conference of Industrial Electronics Society*, Vol.02, pp. 1144-1149, 2002.

[7] R. Naik, T. A. Nondahl, M. J. Melfi, R. Schiferl, J. S. Wang, "Circuit Model For Shaft Voltage Prediction In Induction Motors Fed BY PWM-Based AC Drives", *IEEE Trans. On Industry Applications*, Vol. 39, pp. 1294-1299, Sep./Oct. 2003.

[8] A. Esmaeli, B. Jiang, L. Sun, "Modeling And Suppression Of PWM Inverter's Adverse Effects", *1st International Symposium on Systems and Control in Aerospace and Astronautics*, EI&IEEE, pp. 1450-1454, China, 2006.

[9] L. Arnedo, K. Venkatesan, "P-Spice Simulation For Conducted EMI And Over Voltage Investigations In A PWM Induction Motor Drive System", *IEEE Workshop on Computers in Power Electronics*, pp. 132-137, Jun, 2002.

[10] A. Boglietti, A. Cavagnino, M. Lazzari, "Experimental High Frequency Parameter Identification Of AC Electrical Motors", *IEEE International Conference on Electric Machines and Drives*, pp. 05-10, May, 2005.

[11] H. Akagi, T. Doumoto, "An Approach To Eliminating High-Frequency Shaft Voltage And Ground Leakage Current From An Inverter-Driven Motor", *IEEE Trans. On Industry Applications*, Vol. 40, pp. 1162-1169, Jul./Aug. 2004

[12] Hayt, W. - Buck, J. A. - *Engineering Electromagnetics* - 6th Edition – McGraw - 2001

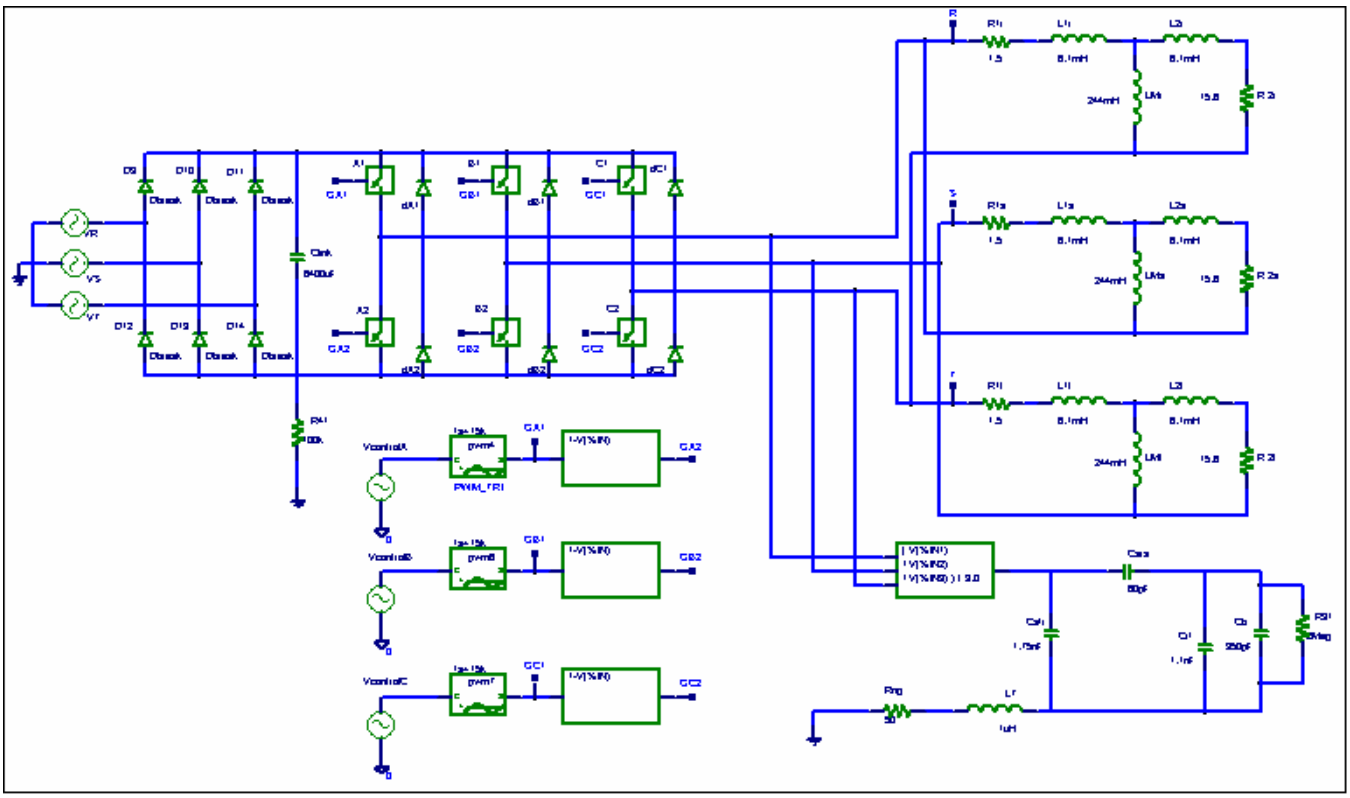

Fig. 8 – Pspice equivalent electrical circuit representation.